Towards chronic deep brain stimulation in freely moving hemiparkinsonian rats: Applicability and functionality of a fully implantable stimulation system

Nadine Apetz[2], Kunal Paralikar[6], Bernd Neumaier[1,2], Alexander Drzezga[3, 7, 8], Dirk Wiedermann[4], Rajesh Iyer[6], Gordon Munns[6], Erik Scott[6], Lars Timmermann[5] and Heike Endepols[1,2,3]

[1]Forschungszentrum Jülich GmbH, Institute of Neuroscience and Medicine, Nuclear Chemistry (INM-5), Wilhelm-Johnen-Straße, 52428 Jülich, Germany
[2]University of Cologne, Faculty of Medicine and University Hospital Cologne, Institute of Radiochemistry and Experimental Molecular Imaging, Kerpener Str. 62, 50937 Köln, Germany
[3]University of Cologne, Faculty of Medicine and University Hospital Cologne, Department of Nuclear Medicine, Kerpener Str. 62, 50937 Köln, Germany
[4]Max Planck Institute for Metabolism Research, Department of In-vivo NMR, Gleueler Str. 50, 50931 Köln, Germany
[5]Department of Neurology, University Hospital of Giessen and Marburg, Baldingerstrasse, 35043 Marburg, Germany
[6]Medtronic, USA
[7] German Center for Neurodegenerative Diseases (DZNE), Bonn-Cologne, Germany,
[8] Institute of Neuroscience and Medicine (INM-2), Molecular Organization of the Brain, Forschungszentrum Jülich, Germany

Abstract

Objective This study aimed at investigating a novel fully implantable deep brain stimulation system and its ability to modulate brain metabolism and behavior through subthalamic nucleus stimulation in a hemiparkinsonian rat model. **Approach** Twelve male rats were unilaterally lesioned with 6-hydroxydopamine in the medial forebrain bundle and received a fully implantable deep brain stimulation system aiming at the ipsilesional subthalamic nucleus. Each rat underwent three cylinder tests to analyze front paw use: A PRE test before any surgical intervention, an OFF test after surgery but before stimulation onset and an ON test under deep brain stimulation. To visualize brain glucose metabolism in the awake animal, two [^{18}F]FDG scans were conducted in the OFF and ON condition. At least four weeks after surgery, an [^{18}F]FDOPA scan was used to check for dopaminergic integrity. **Main results** In general, STN DBS increased [^{18}F]FDG uptake ipsilesionally and decreased it contralesionally. More specifically, bilateral orbitofrontal cortex, ipsilateral caudate putamen, sensorimotor cortex and nucleus accumbens showed significantly higher tracer uptake in ON compared to OFF condition. Contralateral cingulate and secondary motor cortex, caudate putamen, amygdala, hippocampus, retrosplenial granular cortex, superior colliculus, and parts of the cerebellum exhibited significantly higher [^{18}F]FDG uptake in the OFF condition. On the behavioral level, stimulation was able improve use of the contralesional affected front paw suggesting an effective stimulation produced by the implanted system. **Significance** The fully implantable stimulation system developed by us and presented here offers the output of arbitrary user-defined waveforms, patterns and stimulation settings and allows tracer accumulation in freely moving animals. It is therefore a suitable device for implementing behavioral PET studies. It contributes immensely to the possibilities to characterize and unveil the effects and mechanisms of deep brain stimulation offering valuable clues for future improvements of this therapy.

Keywords Parkinson's disease, deep brain stimulation, 6-OHDA rat model, subthalamic nucleus, cylinder test, [^{18}F]FDG PET

1. Introduction

High frequency deep brain stimulation (DBS) of the subthalamic nucleus (STN) as the major target is a safe and highly efficacious therapy that has been well established in the treatment of Parkinson's disease (PD) over the past two decades (1–4). It has been shown to improve dopamine-sensitive motor symptoms and quality of life, while reducing motor response fluctuations, L-DOPA-induced dyskinesia, and drug dose in advanced PD (5–8). But although DBS has revolutionized the treatment of movement disorders like PD or essential tremor and even certain treatment-resistant neuropsychiatric disorders including Tourette syndrome and obsessive compulsive disorder, its exact therapeutic mechanisms of action are still not well understood (9,10). There are several hypotheses as to how and where DBS takes its effects, including the manipulation of neuronal as well as non-neuronal tissue, alteration of transmitter levels and neurochemical signaling, modulation of local and global neuronal network activity, disruption of pathological oscillations, synaptic plasticity, and potentially neuroprotection and neurogenesis (11,12). Nevertheless, more basic research, pre-clinical and clinical studies are needed to further understand the mode of action of DBS in order to improve and further develop this promising technique with regards to non-motor symptoms and closed-loop stimulation (9,13–15).

Animal models are essential in experimental medical science to investigate etiology, mechanisms and symptoms of human diseases as well as new potential therapeutic strategies. For PD, the 6-hydroxydopamine (6-OHDA) rat model has proven to be a valuable tool in understanding the underlying mechanisms of the disease and in the establishment of new therapies (16–20). It belongs to the toxin-induced models and is based on the uni- or bilalateral intracerebral injection of 6-OHDA into the medial forebrain bundle, the substantia nigra pars compacta, or subregions of the caudate-putamen complex. Here, it leads to a selective degeneration of catecholinaminergic neurons that can be limited to dopaminergic neurons by simultaneous application of inhibitors of the noradrenergic system (21–23).

The 6-OHDA rat model has been used to investigate the mechanisms and effects of DBS in PD by numerous groups. However, most of these studies applied only acute stimulation lasting for minutes to hours in animals that were anaesthetized or restrained by cables to external stimulators (24–28). Some studies investigated longer-term stimulation using systems that were fixed on the animals' heads or combining implanted and external parts (29–31). In contrast, DBS in patients is applied continuously over years through a fully implanted system. Thus, the applicability of the results of such studies is limited and there is a great need for animal studies investigating the effects of chronic DBS.

To our knowledge, there is only one other study by Harnack and colleagues that used a fully implantable stimulation system in rats (32). However, their focus was on the safety and integrity of the system rather than on the effects of the stimulation. Hence, the present study aimed at investigating a novel fully implantable DBS system and its ability to modulate brain metabolism and behavior through STN DBS in a hemiparkinsonian rat model. This system allows for stimulation times ranging from seconds to weeks, therefore more realistically mimicking the long-term stimulation as present in PD patients.

2. Materials and Methods

2.1 Animals

Twelve male Long-Evans rats (Janvier Labs, 295 – 425 g) were unilaterally lesioned with 6-OHDA in the medial forebrain bundle and received a fully implantable DBS system aiming at the STN. Animals were kept in groups of two to four in individually ventilated cages (NextGen, Ecoflow, Phantom; Allentown, USA) with free access to standard rodent chow and water. Rats were housed at a reversed day-night-cycle (lights on 8:30 pm to 8:30 am) at a room temperature of 22 ± 1 °C and a relative humidity of 55 ± 5 %.

All experiments took place in the dark (active) phase of the animals at approximately the same time each day to avoid changes caused by their circadian rhythm. Experiments were carried out in accordance with the EU directive 2010/63/EU for animal experiments and the German Animal Welfare Act (TierSchG, 2006) and were approved by regional authorities (LANUV NRW; application number 84-02.04.2012.A304).

2.2 Stimulation System

2.2.1 Electrode

A concentric bipolar electrode (Science Products GmbH, Hofheim, Germany) with a shaft length of 15 mm and a shaft diameter of 75 µm was used. The platinum/iridium core conductor (first contact) had a tip diameter of 3-5 µm and was separated from a small stainless steel tube (second contact) by polyimide tubing. The 15 mm long shaft was also covered by polyimide tubing for insulation. Two insulated wires exited a mount at the end of the shaft, both of which carried 6 mm long male gold plated pin connectors with a diameter of just under 0.79 mm. These pin connectors were compatible with the female pin connectors of the extension leads connecting electrode and stimulator. A schematic illustration of the electrode can be seen in Fig. 1 (b).

2.2.2 Stimulation System

The system for neurostimulation developed by us included a low-volume (~3cc), rechargeable, fully-implantable, hermetic neurostimulator, a recharger, a telemetry module and a four contact connector-module to accommodate the leads. The neurostimulator housed a shared coil for telemetry and recharge, stimulation electronics and the rechargeable battery. To support a broad-range of hypothesis testing, the stimulator was designed to meet and exceed clinical stimulation capabilities including the ability to output arbitrary user-defined waveforms and patterns. The stimulation settings were programmed by a laptop running a LabVIEW based graphical user interface. A telemetry module connected as a USB peripheral to the laptop set up a wireless link between the neurostimulator and the laptop. This module could be held at about 15 cm distance above the animal to communicate with and program the implanted neurostimulator thereby facilitating stimulation adjustment in awake and behaving animals. Inductive recharge via an external primary coil was used to charge depleted rechargeable batteries within the neurostimulator. A recharger-box powered by three AA-size batteries energized the primary coil. The neurostimulator had a unique miniaturized rechargeable battery with capacity of 17 milliampere-hours and employed an anode active material comprised of lithium titanate

for long service life and rapid recharge capability (33). The connector module established a contact between the four stimulation channels and the four proximal contacts of a short pig-tail/lead. The pig-tail/lead had four distal contacts, only the two most distal ones of which were enabled for neurostimulation in this study. The distal end of the lead mated with the silicone sheath carrying the proximal contacts of the extension. The connection was tightened with a set-screw. The extensions were insulated with a thin silicone layer. The distal end of the extension terminated in two female gold plated pin connectors which mated with male gold pin connectors of the electrodes (see Fig. 1 (a) and (b)).

All connecting points between stimulator, extensions and pin connectors were sealed with sterile medical adhesive silicone type A (Silastic®, Dow Corning Corp., Midland, MI, USA). A more detailed description of the technical aspects of the stimulators can be found in a paper published by Paralikar and colleagues (34).

Stimulation currents were charge-balanced, had square waveforms and were always set to a frequency of 130 Hz and a pulse width of 60 µs. The amplitude depended on the individual side effect threshold of each rat.

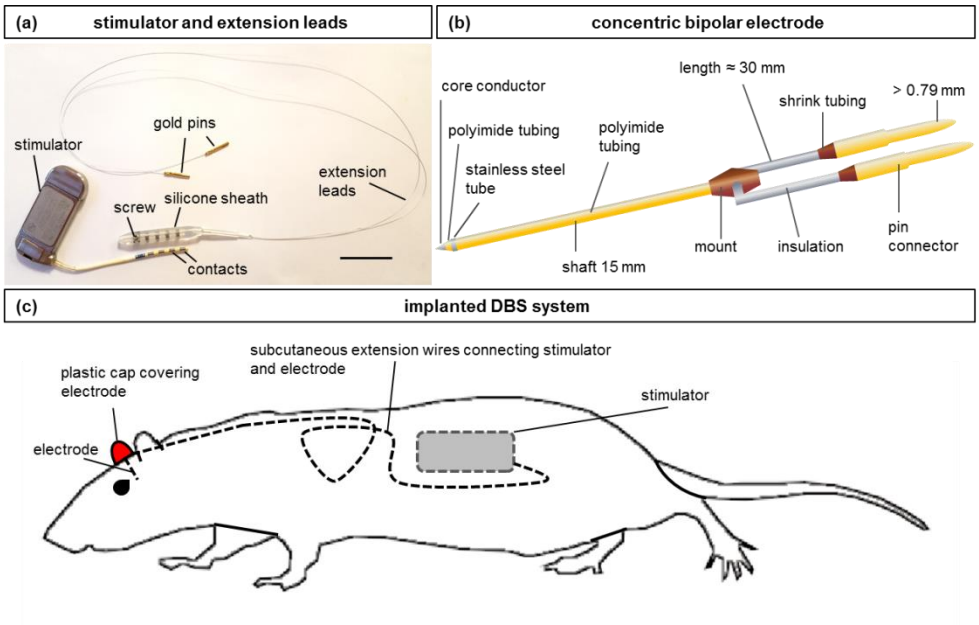

Fig. 1: DBS system. (a) Picture of the implantable stimulator (Medtronic®) and the extension leads (not connected). The leads are connected to the stimulator through a silicone sheath that is put over the contact part and tightened with a screw. The female gold pin connectors of the extension leads match the male pin connectors of the electrode. The stimulator has four contacts, only the two distal ones were used in this study. **(b)** Schematic overview of built and dimensions of the concentric bipolar platinum/iridium electrode that was used for rat subthalamic nucleus deep brain stimulation. The current flows between the core conductor at the tip and the stainless steel tube sitting above it. The electrode is connected to the stimulator via extension leads which plug onto the male gold plated pin connectors. **(c)** Schematic illustration of the implanted DBS system with stimulator, electrode and extension leads. The electrode in the skull is fixated to the bone via plastic screws and a dental cement cap which is the only part of the system not covered by skin. Dashed lines = subcutaneous. The scale bar in (a) represents 2 cm.

2.3 Surgical Procedures

2.3.1 6-OHDA-Lesion and Catheter Implantation

In a first surgery, animals received the 6-OHDA lesion, and a guide cannula (non-metallic mouse guide, 8 mm, PlasticsOne®, San Diego, USA) for the electrode was implanted. Animals were anaesthetized with isoflurane (5 % initiation, 2.5-3.5 % continuation; in a mix of O_2 and aer medicalis, 0.5 and 0.7 l/min, respectively) and fixed on a stereotactic frame. They were placed on a heating plate (Medres® Medical Research GmbH, Cologne, Germany) to maintain body temperature. After reflexes ceased, a subcutaneous injection of 0.1 ml Carprofen (Rimadyl®, Zoetis Deutschland GmbH, Berlin, Germany) was given as analgesic treatment. The top of the head was shaved and wiped with iodine solution for disinfection (Betaisodona®, Mundipharma GmbH, Limburg, Germany). To expose Lambda and Bregma, the skin on the skull was incised longitudinally and clamped to the sides. The skull surface was cleaned with H_2O_2 to better visualise the cranial sutures. A computer assisted stereotactic drill and microinjection robot (Neurostar®, Tübingen, Germany) was used to determine the coordinates of Bregma and Lambda which were used as reference points to appoint the locations of the four drill holes. One hole each was drilled for the guide cannula to the striatum (-3.6 mm posterior, +/-2.8 mm lateral), for the 6-OHDA injection into the medial forebrain bundle (-4.4 mm posterior, +/-1.2 mm lateral) and two more shallow holes for plastic screws (PlasticsOne®, San Diego, USA, nylon mounting screws) to serve as anchors for the dental cement embedding the guide cannula in the end (front screw: +3.0 mm anterior, +/-2.0 mm lateral; back screw: -6.0 mm posterior, +/-2.0 mm lateral). The holes for guide cannula, 6-OHDA lesion and front screw were always on the same side, the hole for the back screw on the other. The side (left or right) of guide cannula and lesion was assigned randomly between animals.

A micro syringe (10 µl, Hamilton®, Bonaduz, Switzerland) was mounted on the stereotactic robot to inject a total of 14 µg of 6-OHDA free base (21 µg of 6-Hydroxydopamine hydrobromide containing ascorbic acid as stabilizer, Sigma Aldrich®, St. Louis, USA) in 3 µl of NaCl at a total depth of 7.9 mm below the dura mater. The syringe was lowered in maximal steps of 1 mm to minimize mechanical lesion and 6-OHDA was injected slowly in steps of 1 µl. The syringe was left in situ for approximately ten minutes to allow for sufficient diffusion of the solution. After removal of the syringe, the hole was closed with bone wax. As a next step, a small manual screw tap was used to prepare the screw holes. Screws were only inserted so far that they held on to the skull without breaching it when possible.

To insert the guide cannula, it was mounted on the stereotactic robot and slowly lowered to a depth of 7.6 mm below the dura mater using the microinjection tool of the robot. The guide cannula was custom built, so that in the final position the tube part was completely inserted and the pedestal part was sitting directly on top of the skull. Subsequently, the pedestal and the screws were embedded in dental cement (Pala® Paladur®, Heraeus Kulzer, Hanau, Germany) to form a little cap keeping the cannula in place. The top half of the pedestal was spared to insert a nylon dummy (PlasticsOne®, San Diego, USA) screwed onto it to cover the opening until the electrode would be inserted. Once the dental cement bonded sufficiently, the skin was sutured as far as possible around the pedestal and the dummy cap. Finally, the wound was treated with iodine solution. Before awakening, each rat received an i.p. injection of approximately 5 ml NaCl to assist circulation and recovery.

2.3.2 Confirmation of Cannula Placement

To verify the correct placement of the guide cannula, and therefore the electrode, an MRI scan was performed before any further procedures. To avoid unnecessary anesthesia sessions and keep animals' stress levels at a minimum it took place either subsequent to the first surgery, or leading up to the second one, in which electrode and stimulator were implanted.

Imaging took place in a 7-T BioSpec 70/20 USR MRI animal scanner (Bruker BioSpin® GmbH, Ettlingen, Germany) equipped with a BGA12S-HP gradient set with a maximum gradient strength of 450 mT/m. RF-coils were used in a cross coil configuration of an actively decoupled linear transmit-only resonator with 7 cm inner diameter and a custom built, anatomically shaped single turn receive-only surface coil of 3 cm diameter. The coil was placed on top of the rats' heads so that the pedestal could extend through its loop. Animals were placed in an MR compatible animal bed (Bruker Biospin) with circulating warm water heating to maintain body temperature at 37 °C. The breathing rate was monitored with a Model 1025 (SA Instruments, Stony Brook, NY, USA) as vitality control and for control and adjustment of the depth of the isoflurane anesthesia.

High resolution anatomical imaging of the site of implantation was done after initial adjustments and acquisition of scout images with a TurboRARE sequence with five slices, slice thickness of 500 µm, a square matrix of 256 x 256 pixel in a field of view of 32 x 32 mm^2 resulting in an in-plane resolution of 125 µm in each direction. TE was set to 12 ms, RARE factor was 8 resulting in an effective TE of 36 ms, TR was set to 5700 ms and 8 averages were acquired to improve the signal-to-noise ratio, resulting in an acquisition time of about 24 min.

MR images were used to determine the individual insertion depth of electrodes for each animal by measuring the distance between tube ending and STN in the image. A stopper was then formed with dental cement at the respective length of each electrode to stop it from sliding through the catheter beyond this point. Electrode placements of all animals are schematically illustrated in Fig. 2 (d).

2.3.3 Electrode and Stimulator Implantation

The day following guide cannula implantation and 6-OHDA lesioning, rats were again anaesthetized as mentioned previously and fixed on the stereotactic frame following the same steps as before. After cessation of reflexes and the injection of Carprofen, an area of about 12 cm^2 was shaved on the left side of rats' backs approximately 2 cm laterally to the spine. The skin was then disinfected with iodine solution and an incision of about 3 cm was made proceeding from dorsal to ventral. Using scissors with rounded tips, a pocket big enough to hold the stimulator was then formed between skin and abdominal wall. The extension cables including the two female gold pins matching the male pin connectors of the electrode were attached to the stimulator which was then inserted into the skin pocket. Subsequently, the suture around the catheter was opened up again and the dental cement cap cleaned and dried. A sharp metal trocar sheathed with a plastic tube was subcutaneously tunneled from the skin pocket holding the stimulator to the opening on the head. The trocar was then removed from the plastic tube, leaving the tube as a subcutaneous tunnel from stimulator to cannula. The extensions holding the female gold pins were lead through the tube to the cannula. The incision on the rats' back was subsequently sutured and treated with iodine solution. Finally, the electrode was

inserted into the cannula and fixed with dental cement. After connecting the two electrode pin connectors with the gold pins coming from the extensions, the whole construction was covered with a small plastic cap and more dental cement until everything was stable and bonded. The suture on the head was closed over the plastic cap and also treated with iodine solution. Finally, animals received an i.p. injection of about 5 ml NaCl to aid circulation and recovery and were placed in their transport box to wake up. Carprofen treatment (0.1 ml/day) continued for three days following the second surgery. Animals were allowed a minimum recovery time of five days.

2.4 Treatment Regimes

2.4.1 Deep Brain Stimulation

Approximately one week after surgeries, following the first baseline [^{18}F]FDG-PET scan and behavioral tests and at least one day before the second [^{18}F]FDG-PET scan, stimulators were turned on.

Stimulation configurations were set at a frequency of 130 Hz, a pulse width of 60 µs, and an initial amplitude of 30 µA. The amplitude was then increased stepwise by 5 µA until side effects like jaw clenching, chewing, apathy or gagging occurred. Animals were then stimulated continuously at 80 % of the determined minimal side effect-evoking amplitude, in this cohort between 40 µA and 220 µA, until completion of the experiment.

2.5 Behavioral Tests

Motor impairment was investigated using the cylinder test which is a fast and simple paradigm that does not require prior training to investigate motor aspects of animal models of disease by looking at the front paw use (35). To this end, animals are placed in a cylinder for several minutes. Their natural curiosity will lead rats to explore the narrow environment by standing on their hind paws, so-called rearing. The number of touches of the cylinder wall with left, right, or both front paws is then recorded. In animal models in which only one body side is affected, e.g. the hemiparkinson model used in this study, animals will touch the cylinder predominantly with the ipsilesional, healthy front paw (IF) while sparing the contralesional affected one (CF). This means that the cylinder test is a suitable test to present unilateral dopamine loss and the involved motor impairment (36), as well as motor recovery caused by STN DBS.

The cylinder used in this study was made of transparent acrylic plastic with a height of 30 cm and a diameter of 20 cm. It was placed under a camera in a dark chamber and could be video-recorded directly from above. On test days, rats were placed in the cylinder for ten minutes. The tracking software The Observer® XT (Noldus, Wageningen, Netherlands) was used for video-analysis in which wall touches of IF, CF and concurrent touches of both paws were counted. The use of CF and IF as a percentage of all wall touches was then calculated. Concurrent contacts were counted as one touch each for IF and CF.

Animals were tested in the cylinder three times: A baseline test was conducted in the naive animal before any surgical intervention (PRE), a second test took place without STN DBS a week after surgery when animals had sufficiently recovered (OFF), and a last test (ON) was done after DBS had been turned on for at least one but a maximum of three days.

2.6 Positron Emission Tomography

PET-scans were performed in a small-animal-PET scanner (Siemens Focus 200, Berlin, Germany). Animals underwent a total of three PET scans: A first [^{18}F]FDG scan about a week after surgeries but before start of STN DBS (OFF) and a second [^{18}F]FDG scan one day after the rats' very first stimulation onset (ON). The third scan was an [^{18}F]FDOPA scan at least four weeks after 6-OHDA injections to verify the dopaminergic lesion.

2.6.1 [^{18}F]FDG

Animals were briefly (< 2 min) anaesthetized with isoflurane as mentioned above to receive an i.p. injection of 73.28 ± 10.55 MBq of [^{18}F]FDG in 0.5 ml saline. [^{18}F]FDG uptake occurred in the awake rat that was allowed to move freely in the cage after waking up. Sixty minutes after the injection, rats were anaesthetized again and a 30 min emission scan was started. During the scan, body temperature was maintained at 37 °C by means of a warm air system integrated in the animal holder (Medres® Medical Research GmbH, Cologne, Germany) and heart rate was continuously monitored. On each PET day, a 10 min transmission scan using a ^{57}Co point source was conducted for attenuation correction. At the end of each scan, blood glucose levels of each rat were measured using a glucose level meter with test strips (Medtronic Contour Link).

2.6.2 [^{18}F]FDOPA

Animals were briefly anaesthetized (< 2 min) and received an i.p. injection of 15 mg/kg benserazide hydrochloride (Sigma Aldrich, St. Louis, USA) to block peripheral decarboxylation of [^{18}F]FDOPA, and thereby increasing central levels. One hour later, animals were anaesthetized again to receive 73.56 ± 7.20 MBq [^{18}F]FDOPA in 0.5 ml saline through a catheter in the lateral tail vein. As with [^{18}F]FDG, animals were placed back in the cage to move freely after [^{18}F]FDOPA injections. 30 min emission scans started half an hour after [^{18}F]FDOPA injection.

2.7 Tissue Processing and Immunohistochemistry

After completion of all behavioral tests and PET sessions, four animals were transcardially perfused with paraformaldehyde (PFA, 4 % in phosphate buffered saline, PBS). The guide cannula including dental cement and electrode was removed from the skull without causing further tissue damage and the brain was extracted. For immunohistological staining, brains were cut at -21 °C in a cryostat (Leica Biosystems, Wetzlar, Germany) in sections of 40 µm and mounted on microscope slides (SuperFrost™ Plus, Thermo Scientific™, Thermo Fisher Scientific, Waltham, USA).

2.7.1 Haematoxylin and Eosin Staining

To check for tissue integrity, especially around the guide cannula and the site of stimulation, sections were stained using Haematoxylin and Eosin. Firstly, slices were covered with PFA (4 % in PBS) for about 10 min. Then, Mayer's Haematoxylin (Lillie's modification, ScyTek Laboratories Inc., Logan, USA) was applied for a maximum of 30 s. They were then incubated in Bluing reagent (ScyTek Laboratories Inc., Logan, USA) for 10-15 s. The excess was blotted off with a rinse in absolute alcohol,

100 % ethanol (EtOH). Slices were then covered with Eosin Y solution (modified alcoholic, ScyTek Laboratories Inc., Logan, USA) for 2-3 min and again washed with absolute alcohol. Following, slices were dehydrated in an ascending alcohol series, i.e. 2 min in 70 %, 96 %, and 100 % EtOH. Finally, they were dipped in Roti®-Histol (Carl Roth GmbH+CoKG, Darmstadt, Germany) for approximately 2 min and immediately cover-slipped with Entellan® rapid mounting medium for microscopy (new, Merck KGaA, Darmstadt, Germany).

2.7.2 TH-Immunohistochemistry

To verify and quantify the unilateral dopaminergic lesion caused by 6-OHDA-injection, the remaining sections were stained for tyrosine hydroxylase (TH) using a monoclonal mouse anti-TH antibody (Sigma-Aldrich, catalogue no. T1299, clone TH-2) as the primary antibody and a horseradish peroxidase (HRP) mouse anti-Immunglobulin (IgG) substrate kit (Vectastain® ABC-Kit, Vector Laboratories Inc., Burlingame, USA). The primary antibody was applied in a concentration of 1:5000 in PBS with 0.1 % normal horse serum overnight. A DAB-precipitation finalized the staining process. A detailed description of the procedure can be found elsewhere (37).

2.8 Statistical Analysis

2.8.1 Behavior

A percentage of the use of CF and IF was calculated from all recorded wall touches. Percentages were arcus-sinus-transformed and differences between CF and IF during PRE, OFF and ON tests were tested for significance ($p \leq 0.05$) with a two-way repeated measures ANOVA using the software Graphpad Prism version 8 for macOS. Factors were paw (CF and IF) and DBS status (PRE, OFF and ON). For post-hoc testing Sidak's multiple comparison test was used.

2.8.2 [^{18}F]FDG PET

After Fourier rebinning, summed images (60–90 min p.i.) were reconstructed using an iterative OSEM3D/MAP procedure (38) resulting in voxel sizes of 0.38 × 0.38 × 0.80 mm. All further analysis was done with the Software VINCI version 4.68 (39). Images were co-registered manually to the Swanson rat brain atlas (40). When lesions were in the right hemisphere, images were flipped so that the intervention was always displayed on the left. Intensity was normalized to the cerebral global mean (standardized uptake value ratio, $SUVR_{wb}$ = individual voxel value divided by mean value of the whole brain).

ON and OFF images were compared voxel-wise using a paired t-test followed by a threshold-free cluster enhancement (TFCE) procedure with subsequent permutation testing (41). This resulted in statistical t-maps corrected for multiple testing, thresholded at $p = 0.05$. As TFCE values are arbitrary, color bars of TFCE maps are labelled with the original t-values, marked t_{TFCE} (Fig 3 (a)).

2.8.3 [^{18}F]FDOPA PET

Images were reconstructed and coregistered as mentioned above. They were smoothed with a Gauss kernel of 1.5 mm FWHM and intensity normalized to the cerebellum ($SUVR_{cer}$ = individual voxel value divided by the mean value of cerebellum). Volumes of interest (VOIs) were drawn of the medial and lateral striatum. Ipsi- versus contralesional mean SUVRs were compared using a paired t-test.

3. Results

3.1 Dopaminergic lesion and electrode placement

Eleven of the twelve rats underwent an [^{18}F]FDOPA PET scan at least four weeks post surgeries to verify the presence of a dopaminergic lesion. Tracer uptake was significantly reduced in ipsilesional striatum ($p = 0.01$; mean $SUVR_{healthy}$: 2.29±0.21, mean $SUVR_{lesioned}$: 2.03±0.21) when compared to its contralateral counterpart (Fig 2 (a)). Dopaminergic integrity was also examined by means of immunohistological staining against TH. As seen in Fig. 2 (b), the ipsilesional striatum barely displays any staining, whereas there is a profound staining in the contralesional hemisphere. Results from [^{18}F]FDOPA PET and immunohistological staining therefore confirm a successful lesion of the dopaminergic system in the basal ganglia caused by the 6-OHDA injection.

Interoperative MRI confirmed the correct placement of the guide cannula (Fig. 2 (c) and (e)). To verify the exact position of electrode tips, histological staining with Haematoxylin and Eosin was applied. Fig. 2 (f) displays the deepest point of the electrode track after careful removal of the electrode targeting the STN. Furthermore, no major tissue damage is visible around the stimulation site implying the safety of the used stimulation system and paradigm. Using MRI and histological sections, the stimulation sites of all eleven animals could be determined and were located in the STN (Fig. 2 (d)).

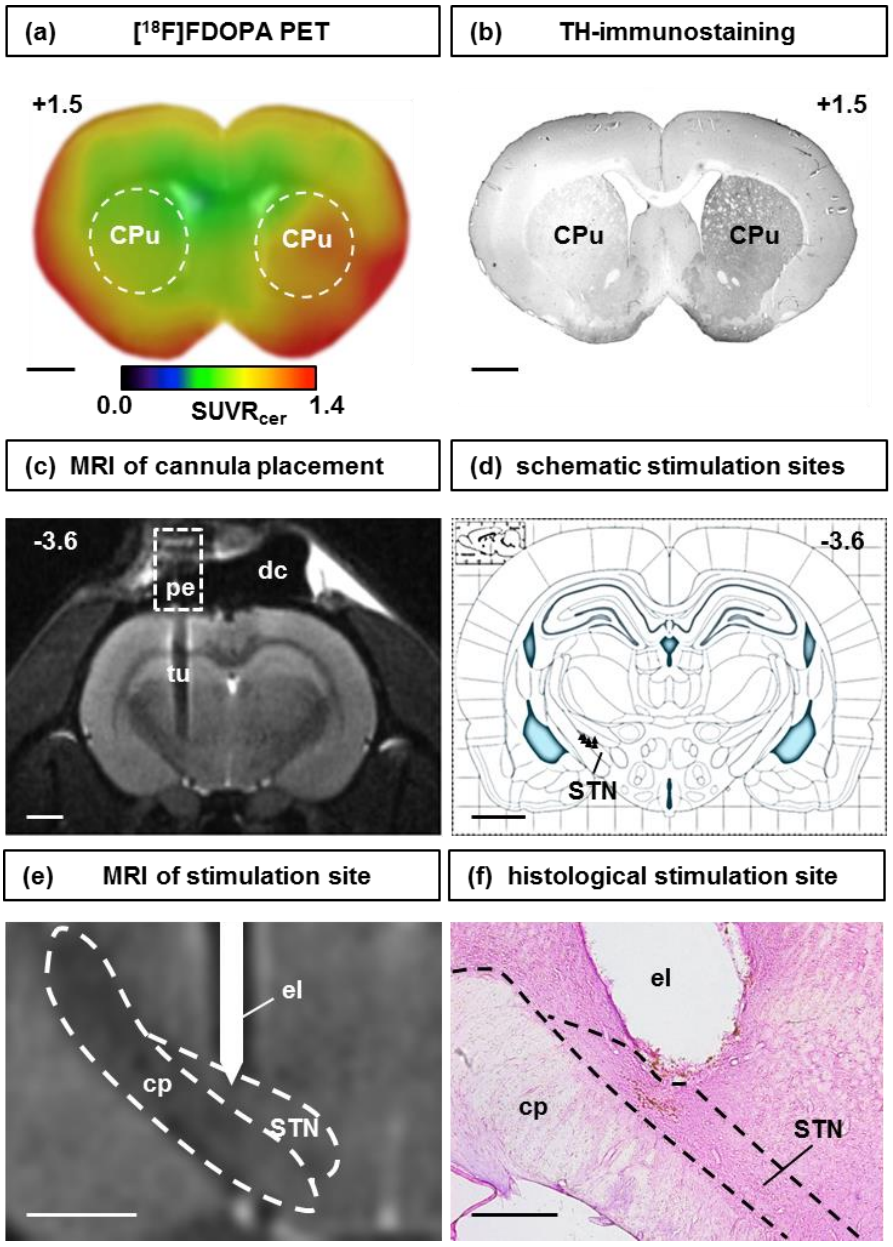

Fig. 2 Dopaminergic lesion and electrode placement. (a) Mean [^{18}F]FDOPA $SUVR_{cer}$ image of animals injected with 6-OHDA in the medial forebrain bundle (n = 11). The dashed lines indicate the striatal areas (caudate putamen, CPu). The left CPu shows a significantly decreased [^{18}F]FDOPA uptake compared to the right striatum. **(b)** Brain slice stained against tyrosine hydroxylase (TH) and precipitated with 3,3'-diaminobenzidine (DAB) with metal enhancer. On the left, lesioned side staining is barely noticeable, whereas there is a profound staining in the right, healthy hemisphere. **(c)** Interoperative MRI taken after implantation of the guide cannula but before the electrode was inserted. The tube (tu) of the guide cannula targets the STN. It is attached to a pedestal (pe) which is fixated on the skull with dental cement (dc). **(d)** Schematic brain atlas (adapted (42)) showing stimulation sites in rats implanted with a DBS electrode. Sites were determined by verifying catheter placements using MRI. **(e)** Detailed image of the stimulation site as seen on the MR image in C. The sketched electrode (el) targets the STN located superior to the cerebral peduncle (pc) which should not be stimulated. **(f)** Histological section stained with Haematoxylin and Eosin showing the stimulation site in detail after removal of the electrode. MR and PET images of animals implanted in the right hemisphere were flipped so that all stimulation sites are shown on the left. The scale bar represents 2 mm in A–E, and 500 µm in F.

3.2 STN DBS effects on behavior

Seven of the twelve rats completed a total of three cylinder tests (see Fig. 3 (a)). A baseline test was conducted before any surgical intervention in the naive rat (PRE). Animals used both paws equally, i.e. the prospective contralesional front paw was used in 51.99 % of all wall touches (see Fig 3 (b)). The two-way repeated measures ANOVA revealed significant main effects for DBS state (PRE, OFF, ON; $F(2,12) = 5.789$, $p = 0.017$) and paw (CF, IF; $F(1,6) = 15.03$, $p = 0.008$) as well as a significant cross-over interaction between DBS state and paw ($F(2,12) = 22.00$, $p \leq 0.0001$). Post-hoc analyses of the main DBS effect (CF and IF pooled) showed that paw use differed significantly between PRE vs. OFF ($p = 0.024$) but not between PRE vs. ON or ON vs. OFF (Fig. 3 (b)). STN DBS (ON) was able to nearly double CF use compared to OFF (OFF: 11.46 % of all wall touches, ON: 20.8 % of all wall touches), indicating an improvement of CF use during STN DBS approaching PRE levels. However, this increase towards OFF was not statistically significant ($p = 0.944$). This could be explained by the large standard deviation of the data set. Animals responded very differently to 6-OHDA lesions; some still explored the cylinder with their impaired front paw to some degree, while others, two animals in particular, stopped moving completely for the duration of the test regardless of the stimulation setting.

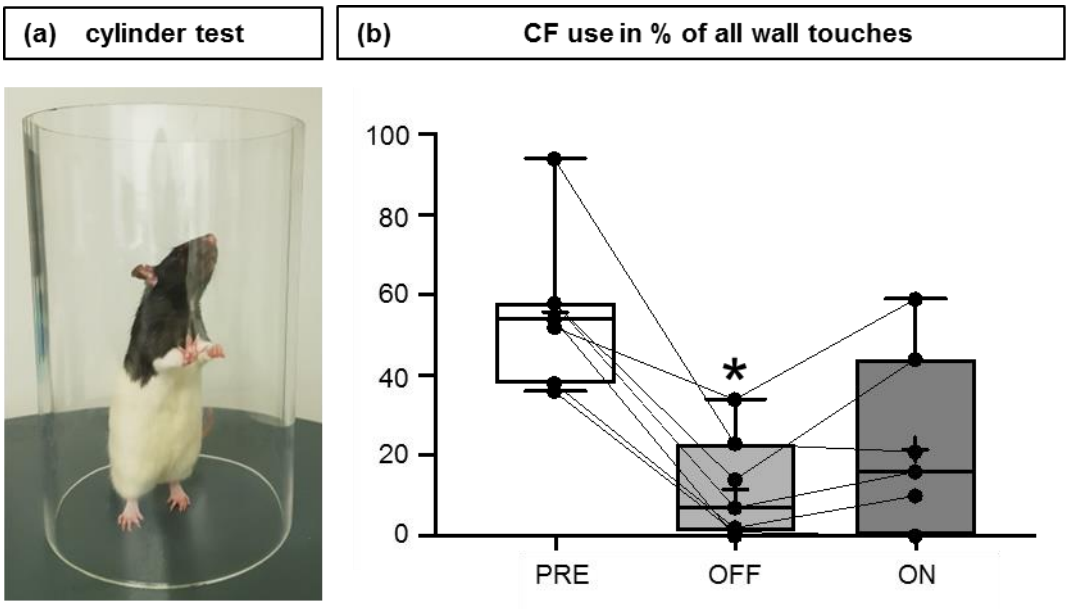

Fig. 3: Cylinder test. (a) Cylinder Test installation. **(b)** Percentage of wall touches with the contralateral, affected front paw (CF) during a 10-min cylinder test (n = 7) before surgery (PRE), post-surgery but before stimulation onset (OFF) and under STN DBS (ON). There was a significant reduction of wall touches with CF after 6-OHDA lesioning (OFF), which was no longer significant during DBS (ON). Asterisk indicates significant difference to PRE.

3.3 STN DBS effects on cerebral [^{18}F]FDG uptake

Eleven rats underwent two [^{18}F]FDG PET scans: one after animals had sufficiently recovered from surgery but before onset of STN DBS, and one under active STN DBS. In general, STN DBS increased [^{18}F]FDG uptake ipsilesionally and decreased it contralesionally. More specifically, bilateral

orbitofrontal cortex, ipsilateral caudate putamen (striatum), parts of the sensorimotor cortex, thalamus, hypothalamus, nucleus accumbens and dorsal subiculum showed significantly higher tracer uptake in ON compared to OFF condition (Fig. 4). Contralateral cingulate and secondary motor cortex, caudate putamen, hypothalamus, ventral pallidum, amygdala, entorhinal cortex, hippocampus, retrosplenial granular cortex, and superior colliculus as well as ipsilateral paraflocculus and parvicellular reticular nucleus exhibited significantly lower [^{18}F]FDG uptake under STN DBS.

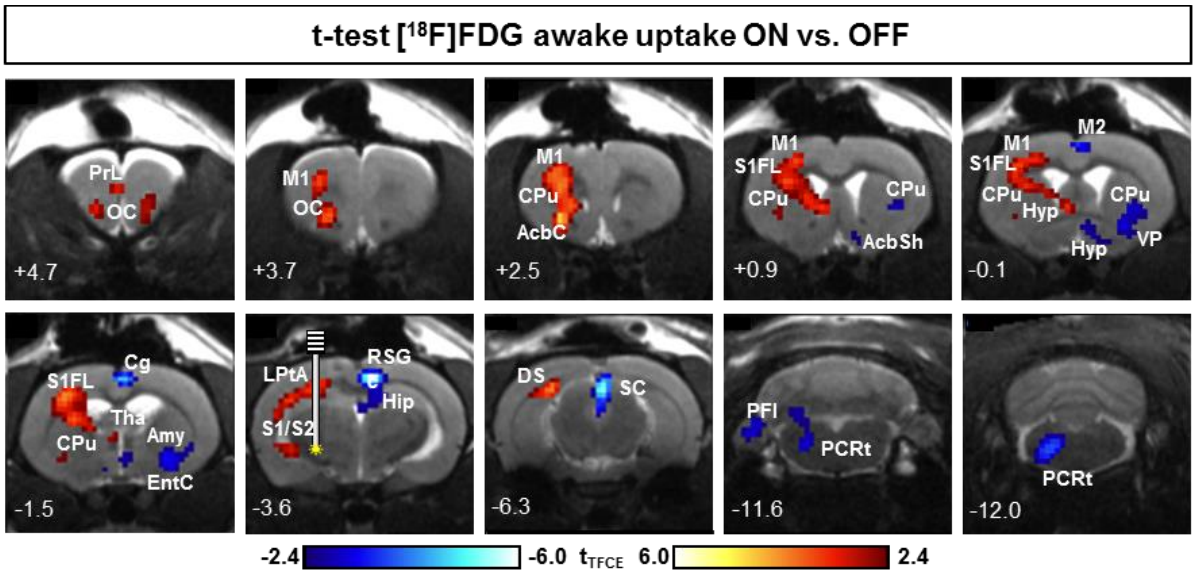

Fig. 4: Effects of DBS on cerebral glucose metabolism. Subtractive t-map ($p < 0.05$, TFCE-corrected) displaying the [^{18}F]FDG uptake difference between DBS ON and OFF in 6-OHDA-injected rats (n = 11). Red voxels indicate that [^{18}F]FDG accumulation was significantly higher during DBS ON, while blue voxels indicate a significantly higher [^{18}F]FDG uptake during DBS OFF. Abbreviations: AcbC = Nucl. accumbens core, AcbSh = Nucl. accumbens shell, Amy = amygdala, Cg = cingulate cortex, CPu = caudate putamen, DS = dorsal subiculum, EnC = entorhinal cortex, Hip = hippocampus, Hyp = hypothalamus, LPtA = lateral parietal association cortex, M1/2 = primary/secondary motor cortex, OC = orbitofrontal cortex, PCRt = parvicellular reticular nucleus, PFl = paraflocculus, PrL = prelimbic cortex, RSG = retrosplenial granular cortex, S1/S2 = primary/secondary somatosensory cortex, S1FL = primary somatosensory cortex forelimb region, SC = superior colliculus, VP = ventral pallidum. PET images of animals implanted in the right hemisphere were flipped so that all stimulation sites are shown on the left. Color bars of TFCE maps are labelled with the original suprathreshold t-values. Numbers indicate rostrocaudal coordinates in mm distance to Bregma.

4. Discussion

The present study aimed to establish an effective, fully implantable DBS system for small rodents that allows for continuous stimulation in an unrestrained and awake animal, a significant improvement over current portable or wireless STN systems for rodents. To test applicability and functionality, we employed the system in a 6-OHDA hemiparkinsonian rat model. Stimulation targeted the STN and its effects were investigated using [^{18}F]FDG PET. Stimulation effects on a behavioral level were tested using a simple cylinder test paradigm.

The implantation of the stimulation system in two separate surgeries as used in this study holds several advantages. First, it mimics the stress on PD patients who commonly receive the electrodes in a first, and the stimulator in a second surgery one to several days later (43). Secondly, it allows for the confirmation of correct guide catheter placement via MRI between surgeries and therefore ensures the exact position of the stimulation electrode that is later inserted. Last, it reduces the duration of anesthesia at a time and, hence, leads to quicker recovery times of animals post-surgery.

Surgeries and implantation systems were well tolerated by animals and no signs of inflammation or indisposition were observed throughout the duration of experiments. The histological investigation of brains also showed no major tissue damage around the site of stimulation or elsewhere, proving the stimulation paradigm to be safe.

The cylinder test is a simple and fast way to investigate front paw use asymmetries in rats (35). The unilateral 6-OHDA lesion and accompanying dopamine loss will cause rats to favor the ipsilateral, unaffected front paw when supporting their weight against the cylinder wall (44). As shown in Fig. 3 (b), rats' CF use decreased significantly from approximately 50 % to 11 % after 6-OHDA lesion. Under STN DBS for 24 h, CF use nearly doubled to about 20 %, losing its significant reduction towards PRE and approaching levels of a naïve animal. The high standard deviation in the ON condition suggests, that animals respond differently to STN DBS. This goes in line with PD patients that show very diverse outcomes of STN DBS and require a thorough selection pre-surgery as well as fine adjustments and programming of the stimulation parameters post-surgery (15). Since there was no readjustment of DBS or additional treatment with dopaminergic drugs throughout the experiments, as practiced in PD patients, some animals might not have received their individual best stimulation settings and therefore underperformed in the cylinder test under STN DBS. In addition, Dowd and Dunnett (2004) showed that hemiparkinsonian rats with a dopamine loss exceeding 95 % exhibit a very robust asymmetry in front paw use that is not always completely reversible by different therapeutic interventions (45). Nevertheless, the improvement of about 18 % for CF use under STN DBS compared to the unstimulated state shown here lies within the same range as seen with improvements of bradykinesia in PD patients (15). Forni and colleagues (2012) showed an improvement of nearly 40 % when comparing double contacts of 6-OHDA rats in the cylinder test before and during STN DBS (31). However, their system was not fully implantable and they applied stimulation for two weeks, which could have reinforced and stabilized the effect. Experiments with chronic STN DBS using the implantable stimulation system introduced here are currently being conducted to compare the effects of acute and chronic DBS. Considering the points made above, the tendency towards an increased CF use in the ON condition suggests an effective STN DBS produced by the implanted system.

[^{18}F]FDG PET scans were used to investigate changes in cerebral glucose consumption caused by unilateral STN DBS. Cell uptake of [^{18}F]FDG is equivalent to cell glucose consumption and reflects mainly synaptic activity (46,47). In a previous investigation, it was shown that unilateral 6-OHDA injections into the medial forebrain bundle cause ipsilesional hypometabolism in striatum and thalamus, and contralesional hypermetabolism in striatum and midbrain locomotor regions (48). A similar hemispherical imbalance in glucose metabolism caused by unilateral 6-OHDA injection into the medial forebrain bundle has also been shown by another rat [^{18}F]FDG PET study (49). In a more

recent work, it was demonstrated using an external stimulation system that STN DBS reverses this metabolic imbalance by increasing [^{18}F]FDG uptake ipsilesionally in ventrolateral striatum and decreasing it contralesionally in thalamus and midbrain (37). These results could largely be repeated in this study using the fully implantable stimulation system. Increases of cerebral metabolism were observed ipsilesionally, while decreases in metabolism were mainly present contralesionally. The activation of the ipsilesional striatal area seems to be a very robust effect under STN DBS as it was also shown by another group using PET (50). Other parallels to this study were a decrease in glucose metabolism of the contralesional entorhinal cortex and amygdala, as well as increases of [^{18}F]FDG uptake in ipsilesional thalamus and caudate putamen. Decreases of glucose consumption of the hippocampus were shown in both analyses. However, in the present work these decreases were contralesional while found ipsilesionally in the study by Jang et al. (2012). Opposite effects were observed for brainstem and cingulate cortex which showed metabolic reductions in our investigation, as well as for somatosensory cortex and prelimbic cortex which exhibited increases in metabolism in the present study.

The conformity of main results between these studies, i.e. ipsilesional metabolic increases, especially in the striatum, and contralesional decreases, confirm the applicability of the fully implantable stimulation system used here. However, the slight discrepancies found throughout the studies mentioned above demonstrate the great lack of PET experiments looking at and further characterizing STN DBS induced effects on cerebral metabolism and network functioning in hemiparkinsonian rats. The present study showed for the first time that a fully implantable neurostimulation system for rodents is a useful tool to investigate changes in behavior as well as in brain metabolism caused by DBS when combined with [^{18}F]FDG PET in a rat hemiparkinsonian model. As mentioned earlier, experiments comparing acute and chronic STN DBS with stimulation times of five weeks using the system introduced here are already underway. Future studies in this area should now focus on chronic DBS and its effects using behavioral PET to elucidate the specific cerebral network mechanisms during healthy, impaired and DBS-treated movement in more detail. Different current waveforms, patterns and stimulation settings also need to be tested as it is done in clinical use. The stimulation system presented here offers the output of arbitrary user-defined waveforms, patterns and stimulation settings and allows tracer accumulation in awake and unrestrained animals. Its great advantage towards DBS-systems currently used in rodent studies is that it is fully implantable. External or partly implanted stimulation systems require single housing of animals or even specialized cages to minimize the chance of system damage (30,31). Animals in this study could be housed in groups in standard cages, allowing for natural behaviors such as grooming, playing and other social activities. A study by Pinnell et al. (2018) observed an ultra-small DBS system in pair-housed rats for eight days (29). However, actual stimulation times did not exceed one hour daily. Due to its inductive charging, our DBS system offers unlimited stimulation time. It is not clear, at present, whether chronic stimulation times exceeding that reached with other systems lead to different findings regarding behavior or brain metabolism, e.g. habituation or further improvements. Nevertheless, the DBS system presented here holds the possibility to find out while not being limited by special housing or experimental requirements. It is therefore a suitable device for implementing behavioral PET studies. Hence, it

contributes immensely to the possibilities to characterize and unveil the effects and mechanisms of DBS and offers valuable clues for future improvements of DBS therapy.

Acknowledgements

This work was funded by the German Science Foundation (DFG), KFO 219, grant number EN 439/4-1. HE, LT and NA designed the study. NA and HE performed animal experiments. KP, RI, GM and ES are employees of Medtronic.,Inc. They developed and provided the stimulation system. DW gave technical support concerning the MR. NA and HE analyzed the data. BN and AD provided the PET tracers. NA wrote the manuscript. All authors discussed the data and edited the manuscript.

References

1. Benabid A L, Pollak P, Gross C, Hoffmann D, Benazzouz A, Gao D M, Laurent A, Gentil M, Perret J 1995 Acute and long-term effects of subthalamic nucleus stimulation in Parkinson's disease *Stereotact. Funct. Neurosurg.* **62** 76–84

2. Limousin P, Pollak P, Benazzouz A, Hoffmann D, Le Bas J-F, Perret J E, Benabid A-L, Broussolle E 1995 Effect on parkinsonian signs and symptoms of bilateral subthalamic nucleus stimulation *The Lancet* **345** 91–5

3. Benazzouz A, Gross C, Féger J, Boraud T, Bioulac B 1993 Reversal of rigidity and improvement in motor performance by subthalamic high-frequency stimulation in MPTP-treated monkeys *Eur. J. Neurosci.* **5** 382–9

4. Bergman H, Wichmann T, DeLong M R 1990 Reversal of experimental parkinsonism by lesions of the subthalamic nucleus *Science* **249** 1436–8

5. Moro E, Scerrati M, Romito L M A, Roselli R, Tonali P, Albanese A 1999 Chronic subthalamic nucleus stimulation reduces medication requirements in Parkinson's disease *Neurology* **53** 85–85

6. Limousin P, Krack P, Pollak P, Benazzouz A, Ardouin C, Hoffmann D, Benabid A-L 1998 Electrical stimulation of the subthalamic nucleus in advanced Parkinson's disease *N. Engl. J. Med.* **339** 1105–11

7. Kumar R, Lozano A M, Kim Y J, Hutchison W D, Sime E, Halket E, Lang A E 1998 Double-blind evaluation of subthalamic nucleus deep brain stimulation in advanced Parkinson's disease *Neurology* **51** 850–5

8. Vingerhoets F J G, Villemure J-G, Temperli P, Pollo C, Pralong E, Ghika J 2002 Subthalamic DBS replaces levodopa in Parkinson's disease: Two-year follow-up *Neurology* **58** 396–401

9. Udupa K, Chen R 2015 The mechanisms of action of deep brain stimulation and ideas for the future development *Prog. Neurobiol.* **133** 27–49

10. Martinez-Ramirez D, Hu W, Bona A R, Okun M S, Shukla A W 2015 Update on deep brain stimulation in Parkinson's disease *Transl. Neurodegener.* **4** 12

11. McIntyre C C, Anderson R W 2016 Deep brain stimulation mechanisms: the control of network activity via neurochemistry modulation *J. Neurochem.* **139** 338-345

12. Herrington T M, Cheng J J, Eskandar E N 2016 Mechanisms of deep brain stimulation *J. Neurophysiol.* **115** 19–38

13. Faggiani E, Benazzouz A 2016 Deep brain stimulation of the subthalamic nucleus in Parkinson's disease: From history to the interaction with the monoaminergic systems *Prog. Neurobiol.* **151** 139–56

14. Kühn A A, Volkmann J 2016 Innovations in deep brain stimulation methodology *Mov. Disord. Off. J. Mov. Disord. Soc.* **32** 11-19

15. Benabid A L, Chabardes S, Mitrofanis J, Pollak P 2009 Deep brain stimulation of the subthalamic nucleus for the treatment of Parkinson's disease *Lancet Neurol.* **8** 67–81

16. Mackovski N et al. 2016 Reversal effect of simvastatin on the decrease in cannabinoid receptor 1 density in 6-hydroxydopamine lesioned rat brains *Life Sci.* **155** 123–32

17. Noor N A, Mohammed H S, Mourad I M, Khadrawy Y A, Aboul Ezz H S 2016 A promising therapeutic potential of cerebrolysin in 6-OHDA rat model of Parkinson's disease *Life Sci.* **155** 174–9

18. Shi K, Liu X, Qiao D, Hou L 2017 Effects of treadmill exercise on spontaneous firing activities of striatal neurons in a rat model of Parkinson's disease *Motor Control.* **21** 58–71

19. Wang X, Yang H A, Wang X N, Du Y F 2016 Effect of siRNA-induced silencing of cellular prion protein on tyrosine hydroxylase expression in the substantia nigra of a rat model of Parkinson's disease *Genet. Mol. Res.* **15** gmr.15027406

20. Wang Z-Y, Lian H, Zhou L, Zhang Y-M, Cai Q-Q, Zheng L-F, Zhu J-X 2016 Altered expression of D1 and D2 dopamine receptors in vagal neurons innervating the gastric muscularis externa in a Parkinson's disease rat model *J. Park. Dis.* **6** 317–23

21. Deumens R, Blokland A, Prickaerts J 2002 Modeling parkinson's disease in rats: an evaluation of 6-ohda lesions of the nigrostriatal pathway *Exp. Neurol.* **175** 303–17

22. Gerlach M, Riederer P 1996 Animal models of Parkinson's disease: An empirical comparison with the phenomenology of the disease in man *J. Neural. Transm.* **103** 987–1041

23. Betarbet R, Sherer T B, Greenamyre J T 2002 Animal models of Parkinson's disease *BioEssays.* **24** 308–18

24. Dorval A D, Grill W M 2014 Deep brain stimulation of the subthalamic nucleus reestablishes neuronal information transmission in the 6-OHDA rat model of parkinsonism *J. Neurophysiol.* **111** 1949–59

25. He Z, Jiang Y, Xu H, Jiang H, Jia W, Sun P, Xie J 2014 High frequency stimulation of subthalamic nucleus results in behavioral recovery by increasing striatal dopamine release in 6-hydroxydopamine lesioned rat *Behav. Brain. Res.* **263** 108–14

26. Lindemann C, Krauss J K, Schwabe K 2012 Deep brain stimulation of the subthalamic nucleus in the 6-hydroxydopamine rat model of Parkinson's disease: Effects on sensorimotor gating *Behav. Brain Res.* **230** 243–50

27. Shi L-H, Woodward D J, Luo F, Anstrom K, Schallert T, Chang J-Y 2004 High-frequency stimulation of the subthalamic nucleus reverses limb-use asymmetry in rats with unilateral 6-hydroxydopamine lesions *Brain Res.* **1013** 98–106

28. Temel Y, Visser-Vandewalle V, Aendekerk B, Rutten B, Tan S, Scholtissen B, Schmitz C, Blokland A, Steinbusch H W M 2005 Acute and separate modulation of motor and cognitive

performance in parkinsonian rats by bilateral stimulation of the subthalamic nucleus *Exp. Neurol.* **193** 43–52

29. Pinnell R C, Pereira de Vasconcelos A, Cassel J C, Hofmann U G 2018 A Miniaturized, Programmable Deep-Brain Stimulator for Group-Housing and Water Maze Use *Front. Neurosci.* **12** 231

30. Alpaugh M, Saint-Pierre M, Dubois M, Aubé B, Arsenault D, Kriz J, Cicchetti A, Cicchetti F 2019 A novel wireless brain stimulation device for long-term use in freely moving mice *Sci. Rep.* **9** 1–10

31. Forni C, Mainard O, Melon C, Goguenheim D, Kerkerian-Le Goff L, Salin P 2012 Portable microstimulator for chronic deep brain stimulation in freely moving rats *J. Neurosci. Methods* **209** 50–7

32. Harnack D, Meissner W, Paulat R, Hilgenfeld H, Müller W-D, Winter C, Morgenstern R, Kupsch A 2008 Continuous high-frequency stimulation in freely moving rats: Development of an implantable microstimulation system *J. Neurosci. Methods* **167** 278–91

33. Eberman K, Gomadam P, Jain G, Scott E 2010 Material and Design Options for Avoiding Lithium Plating during Charging *ECS Trans.* **25** 47–58

34. Paralikar K, Santa W, Iyer R, Thom A, Su X, Hovland E, Dinsmoor D, Munns G, May S, Scott E, Denison T 2015 A fully implantable and rechargeable neurostimulation system for animal research *7th International IEEE/EMBS Conference on Neural Engineering (NER)* 418–21

35. Schallert T, Tillerson J L 2000 Intervention Strategies for Degeneration of Dopamine Neurons in Parkinsonism *Central Nervous System Diseases: Innovative Animal Models from Lab to Clinic* ed D F Emerich, R L Dean, P R Sanberg (Totowa, NJ: Humana Press) 131–51

36. Schallert T, Fleming S M, Leasure J L, Tillerson J L, Bland S T 2000 CNS plasticity and assessment of forelimb sensorimotor outcome in unilateral rat models of stroke, cortical ablation, parkinsonism and spinal cord injury *Neuropharmacology* **39** 777–87

37. Apetz N, Kordys E, Simon M, Mang B, Aswendt M, Wiedermann D, Neumaier B Drzezga A, Timmermann L, Endepols H 2019 Effects of subthalamic deep brain stimulation on striatal metabolic connectivity in a rat hemiparkinsonian model *Dis. Model Mech.* **12** dmm039065

38. Qi J, Leahy R M, Cherry S R, Chatziioannou A, Farquhar T H 1998 High-resolution 3D Bayesian image reconstruction using the microPET small-animal scanner *Phys. Med. Biol.* **43** 1001–13

39. Vollmar S, Hampl J A, Kracht L, Herholz K 2007 Integration of functional data (PET) into brain surgery planning and neuronavigation *Advances in Medical Engineering* (Berlin, Heidelberg: Springer) 98–103

40. Swanson L W 1998 *Brain maps : structure of the rat brain : a laboratory guide with printed and electronic templates for data, models and schematics* (Amsterdam, Oxford: Elsevier)

41. Smith S, Nichols T 2009 Threshold-free cluster enhancement: Addressing problems of smoothing, threshold dependence and localisation in cluster inference *NeuroImage* **44** 83–98

42. Paxinos G, Watson C 2005 The rat brain in stereotaxic coordinates (Oxford: Elsevier Academic Press)

43. Machado A, Rezai A R, Kopell B H, Gross R E, Sharan A D, Benabid A-L 2006 Deep brain stimulation for Parkinson's disease: Surgical technique and perioperative management *Mov. Disord.* **21** 247–58

44. Rattka M, Fluri F, Krstić M, Asan E, Volkmann J 2016 A novel approach to assess motor outcome of deep brain stimulation effects in the hemiparkinsonian rat: Staircase and cylinder test *J. Vis. Exp.* **111** e53951

45. Dowd E, Dunnett S B 2004 Deficits in a lateralized associative learning task in dopamine-depleted rats with functional recovery by dopamine-rich transplants *Eur. J. Neurosci.* **20** 1953–9

46. Magistretti P J, Pellerin L 1999 Cellular mechanisms of brain energy metabolism and their relevance to functional brain imaging *Philos. Trans. R. Soc. Lond. B. Biol. Sci.* **354** 1155–63

47. Jueptner M, Weiller C 1995 Review: does measurement of regional cerebral blood flow reflect synaptic activity? Implications for PET and fMRI *NeuroImage* **12** 148–56

48. Kordys E et al. 2017 Motor impairment and compensation in a hemiparkinsonian rat model: correlation between dopamine depletion severity, cerebral metabolism and gait patterns *EJNMMI Res.* **7** 68

49. Jang D P et al. 2012 Functional neuroimaging of the 6-OHDA lesion rat model of Parkinson's disease *Neurosci. Lett.* **513** 187–92

50. Klein J, Soto-Montenegro M L, Pascau J, Günther L, Kupsch A, Desco M, Winter C 2011 A novel approach to investigate neuronal network activity patterns affected by deep brain stimulation in rats *J. Psychiatr. Res.* **45** 927–30